Electrochemistry of Ruthenium Carbonyls

John E. Cyr† and Philip H. Rieger*

Department of Chemistry, Brown University, Providence, Rhode Island 02912

Received December 28, 1990

The electrochemical reduction of $Ru_3(CO)_{12}$ in acetone and dichloromethane solutions was studied by using polarography and cyclic voltammetry. Evidence is presented which suggests that the irreversible two-electron process proceeds via an EE mechanism with opening of the triruthenium ring concerted with the first electron-transfer step. The reduction product, presumed to be open-chain $Ru_3(CO)_{12}^{2-}$, is very rapidly consumed by a second-order process to give $Ru_3(CO)_{11}^{2-}$ and by a competing first-order process to give a species, possibly an acetone adduct, which then slowly decays to $Ru_3(CO)_{11}^{2-}$. The electrochemical oxidations of $Ru(CO)_5$, $Ru_3(CO)_{11}^{2-}$, and $Ru_6(CO)_{18}^{2-}$ were also studied in acetone solution, and cyclic voltammetric data are described.

Introduction

Our interest in ruthenium carbonyls began with the discovery[1] that $Ru_3(CO)_{12}$ is an excellent substrate for electron-transfer chain (ETC) catalyzed nucleophilic substitution reactions. The substitution of a phosphine ligand for CO is fast and efficient when the reaction is initiated by addition of a catalytic amount of benzophenone ketyl to a THF solution of $Ru_3(CO)_{12}$ and the Lewis base. Furthermore, in marked contrast with thermally activated nucleophilic substitution,[2] where the major product is $Ru_3(CO)_9L_3$, mono-, di-, or trisubstitution products were obtained from the ETC reaction, depending on the phosphine:substrate mole ratio. This behavior suggested that the radical anion $Ru_3(CO)_{12}^{\bullet-}$ while reactive toward nucleophiles, was relatively stable as an intermediate in the ETC reaction, a conclusion apparently supported by the observation of an ESR signal, attributed to the radical anion, in THF solutions of $Ru_3(CO)_{12}$, which had been reduced by sodium at low temperatures.[3]

Early electrochemical work on the reduction of $Ru_3(CO)_{12}$ was interpreted in terms of a chemically and electrochemically irreversible one-electron reduction.[4,5] More recently, however, we showed that $Ru_3(CO)_{12}$ undergoes a chemically irreversible two-electron reduction at a Pt cathode in acetone solution.[6] The intermediate radical anion is very rapidly reduced at the electrode surface so that ETC reactions cannot be initiated efficiently at an electrode. A careful electrochemical study of $Ru_3(CO)_{12}$ in CH_2Cl_2, THF, and CH_3CN by Robinson and co-workers[7] verified our general conclusions.

Shore et al.[8] found that anionic clusters were formed when $Ru_3(CO)_{12}$ was reduced with benzophenone ketyl with the product determined by the Ph_2CO^-:$Ru_3(CO)_{12}$ ratio: $Ru_6(CO)_{18}^{2-}$ (1:1), $Ru_4(CO)_{13}^{2-}$ (3:2), $Ru_2(CO)_{11}^{2-}$ (2:1), $Ru_4(CO)_{12}^{4-}$ (3:1). In both our cyclic voltammograms[6] and those of Robinson et al.[7] the reverse trace following reduction of $Ru_3(CO)_{12}$ showed anodic features that could be assigned to the oxidation of two of these anions: $Ru_3(CO)_{11}^{2-}$ and $Ru_6(CO)_{18}^{2-}$.

Although we had no direct evidence, both we and Robinson et al. assumed that the initial product of the two-electron reduction of $Ru_3(CO)_{12}$ is the open-chain dianion, $Ru_3(CO)_{12}^{2-}$, resulting from Ru–Ru bond cleavage in the anion radical. Heinze and co-workers[9] have shown that reduction of $MeCCo_3(CO)_9$ results in loss of a CO ligand from the anion radical and not Co–Co bond cleavage (as we had assumed[10]). A CO-loss mechanism is not operative in the case of $Ru_3(CO)_{12}$, since the putative product, *triangulo*-$Ru_3(CO)_{11}^{2-}$, while formed, clearly arises from secondary reactions (vide infra). Furthermore, substitution of some of the carbonyl ligands by bridging allyl, allenyl, or alkynyl groups[5,11] stabilizes the radical anion intermediate as expected if Ru–Ru bond cleavage is the decay mode.

In cyclic voltammograms of $Ru_3(CO)_{12}$ in acetone, the reverse trace following reduction revealed an anodic peak at ca. –0.1 V, which we assigned to the open-chain dianion. Robinson et al. did not see this feature but found an anodic peak at ca. –0.6 V in cyclic voltammograms of 0.12 mM $Ru_3(CO)_{12}$ in carefully dried CH_2Cl_2, which they assigned to the open-chain dianion. The –0.6-V peak disappeared at higher concentrations or in the presence of traces of moisture, suggesting that the species responsible is consumed by a fast second-order reaction and by a reaction with water. Osella et al.[11] have suggested that the –0.6-V peak might be due to a solvated $Ru(CO)_2$ species, but this assignment is not consistent with Robinson's results. We will show that oxidation of the initially formed reduction product is expected in the range –0.6 to –0.8 V, consistent with Robinson's assignment.

In this paper, we extend the evidence and arguments briefly outlined in our preliminary report and discuss the detailed mechanism of the primary reduction and the ensuing chemical reaction steps. We also report some

† Present address: The Squibb Institute for Medical Research, Box 191, Bldg. 74T, New Brunswick, NJ 08903.

(1) Bruce, M. I.; Kehoe, D. C.; Matisons, J. G.; Nicholson, B. K.; Rieger, P. H.; Williams, M. L. *J. Chem. Soc., Chem. Commun.* **1982**, 442–444. Bruce, M. I.; Matisons, J. G.; Nicholson, B. K. *J. Organomet. Chem.* **1983**, *247*, 321–343. Arewgoda, M.; Robinson, B. H.; Simpson, J. *J. Am. Chem. Soc.* **1983**, *105*, 1893–1903.

(2) Malik, S. K.; Poë, A. *Inorg. Chem.* **1978**, *17*, 1484–1488.

(3) Peake, B. M.; Robinson, B. H.; Simpson, J.; Watson, D. J. *J. Chem. Soc., Chem. Commun.* **1974**, 945–946. Dawson, P. A.; Peake, B. M.; Robinson, B. H.; Simpson, J. *Inorg. Chem.* **1980**, *19*, 465–472.

(4) Bond, A. M.; Dawson, P. A.; Peake, B. M.; Robinson, B. H.; Simpson, J. *Inorg. Chem.* **1977**, *16*, 2199–2206. See also: Peake, B. M.; Robinson, B. H.; Simpson, J.; Watson, D. J. *J. Chem. Soc., Chem. Commun.* **1974**, 945.

(5) Zanello, P.; Aime, S.; Osella, D. *Organometallics* **1984**, *3*, 1374–1378.

(6) Cyr, J. E.; DeGray, J. A.; Gosser, D. K.; Lee, E. S.; Rieger, P. H. *Organometallics* **1985**, *4*, 950–951.

(7) Downard, A. J.; Robinson, B. H.; Simpson, J.; Bond, A. M. *J. Organomet. Chem.* **1987**, *320*, 363–384.

(8) Bhattacharyya, A. A.; Nagel, C. C.; Shore, S. G. *Organometallics* **1983**, *2*, 1187–1193.

(9) Hinkelmann, K.; Heinze, J.; Schacht, H.-T.; Field, J. S.; Vahrenkamp, H. *J. Am. Chem. Soc.* **1989**, *111*, 5078–5091.

(10) Bezems, G. J.; Rieger, P. H.; Visco, S. *J. Chem. Soc., Chem. Commun.* **1981**, 265–266.

(11) Osella, D.; Arman, G.; Gobetto, R.; Laschi, F.; Zanello, P.; Ayrton, S.; Goodfellow, V.; Housecroft, C. E.; Owen, S. M. *Organometallics* **1989**, *8*, 2689–2695.

0276-7333/91/2310-2153$02.50/0

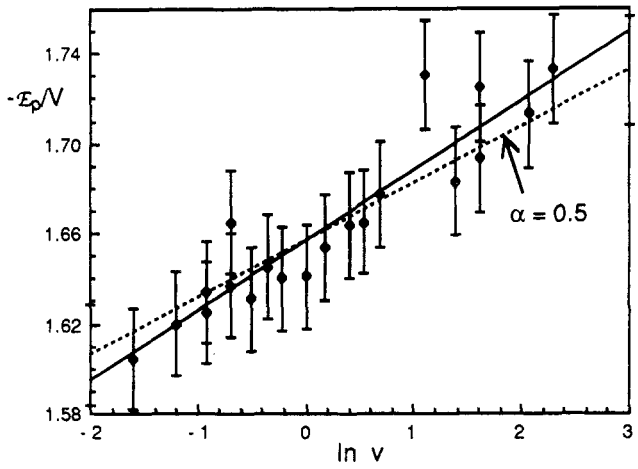

Figure 1. Plot of $Ru_3(CO)_{12}$ reduction peak potential (vs ferrocene) vs the logarithm of the scan rate in volts per second. The solid line corresponds to the least-squares fit with $\alpha = 0.41$; the dashed line corresponds to $\alpha = 0.5$.

electrochemical data on the oxidation of $Ru(CO)_5$, $Ru_3(CO)_{11}^{2-}$, and $Ru_6(CO)_{18}^{2-}$.

Results and Discussion

Reduction of $Ru_3(CO)_{12}$. The reduction of *triangulo*-$Ru_3(CO)_{12}$ involves two electrons overall[6,7] and apparently leads initially to the open-chain dianion, $Ru_3(CO)_{12}^{2-}$. The detailed mechanism of reduction thus involves the transfer of two electrons and opening of the triruthenium ring. A single two-electron wave requires that the standard potential for the second step be greater than or equal to that of the first step, $\Delta E = E_2^\circ - E_1^\circ \geq 0$. In general, we expect that, if an electron-acceptor molecule retains its original conformation, ΔE should be negative, reflecting electron repulsion in the molecular orbital containing the added electrons. Thus it seems most likely that the ring-opening step occurs either after transfer of the first electron (an ECE mechanism) or concerted with transfer of the first electron (an EE mechanism with the first step rate-limiting).

For the ECE mechanism, Scheme I, with ΔE greater than about 100 mV, the cathodic peak potential in a cyclic voltammogram should be that expected for an EC process[12,13]

$$E_p = E_1^\circ - \frac{RT}{2F}\left[1.56 + \ln \frac{Fv}{kRT}\right] \quad (1)$$

where v is the potential scan rate. A plot of E_p vs ln v thus should give a straight line.

Scheme I

$$\textit{triangulo}\text{-}Ru_3(CO)_{12} + e^- \overset{E_1^\circ}{\rightleftharpoons} \textit{triangulo}\text{-}Ru_3(CO)_{12}^{\bullet -}$$

$$\textit{triangulo}\text{-}Ru_3(CO)_{12}^{\bullet -} \xrightarrow{k} Ru_3(CO)_{12}^{\bullet -}$$

$$Ru_3(CO)_{12}^{\bullet -} + e^- \overset{E_2^\circ}{\rightleftharpoons} Ru_3(CO)_{12}^{2-}$$

Peak potentials were measured for acetone solutions containing 1 mM $Ru_3(CO)_{12}$, 1 mM ferrocene, and 0.1 M tetra-*n*-butylammonium perchlorate at various scan rates and corrected for iR drop, with R computed from the separation of the ferrocene anodic and cathodic peaks. A satisfactorily linear plot of E_p vs ln v was obtained, as shown in Figure 1, for $0.2 \leq v \leq 10$ V s^{-1}. For scan rates less than 0.2 V s^{-1}, the data show more scatter, but it appears that E_p approaches an asymtotic value of ca. −1.5 V vs ferrocene. The slope of the linear region is (31 ± 3) mV, considerably greater than that expected from eq 1, $RT/2F$ (12.6 mV at 20 °C).

For an EE process, Scheme II, with the first step rate-limiting and the second step assumed reversible ($\Delta E > 100$ mV), the predicted peak potential is given by[13,14]

$$E_p = E_1^\circ - \frac{RT}{2\alpha F}\left(1.56 + 2 \ln \frac{D^{1/2}}{k_0} + \ln \frac{\alpha F v}{RT}\right) \quad (2)$$

Scheme II

$$\textit{triangulo}\text{-}Ru_3(CO)_{12} + e^- \overset{E_1^\circ}{\rightleftharpoons} Ru_3(CO)_{12}^{\bullet -}$$

$$Ru_3(CO)_{12}^{\bullet -} + e^- \overset{E_2^\circ}{\rightleftharpoons} Ru_3(CO)_{12}^{2-}$$

where k_0 is the electron-transfer rate constant and α is the cathodic transfer coefficient for the rate-limiting step. Equation 2 also predicts that a plot of E_p vs ln v should be linear, but the expected slope is $RT/2\alpha F$, consistent with the experimental result if $\alpha = 0.41 \pm 0.04$, where the error limit corresponds to the standard deviation. The data are sufficiently scattered, however, that $\alpha = 0.5$ is also possible, as shown by the dashed line in Figure 1. The intercept of the E_p vs ln v plot at ln $v = 0$ gives

$$E_1^\circ - \frac{RT}{2\alpha F}\left[1.56 + 2 \ln \frac{D^{1/2}}{k_0} + \ln \frac{\alpha F}{RT}\right] = -1.656 \pm 0.004 \text{ V} \quad (3)$$

The peak potential is expected to level off at very slow scan rates to $E_p = E^\circ - 1.109RT/nF$ where $E^\circ = (E_1^\circ + E_2^\circ)/2$ and $n = 2$. Digital simulation studies show that the linear behavior predicted by eq 2 is expected for

$$E_p \leq E^\circ - \frac{RT}{\alpha F}(1.39 + \ln \alpha^{1/2}) \quad (4)$$

Since the linear region extends down to $v \approx 0.2$ V s^{-1}, we can substitute α and $E_p = -1.60$ V (the peak potential at 0.2 V s^{-1}) into eq 4, to obtain an estimate of $E^\circ \approx -1.54$ V.

A completely irreversible polarographic wave with the first electron-transfer step rate-limiting is expected to be symmetrical with $E_{1/4} - E_{3/4} = 51.7/\alpha$ mV at 20 °C,[15] about 103 mV if $\alpha \approx 0.5$. Although broader than expected for a reversible process, the experimental wave has $E_{1/4} - E_{3/4} \simeq 94$ mV (for $t_d = 1$ s) and is noticeably unsymmetrical. This suggests that on the polarographic time scale the reduction of $Ru_3(CO)_{12}$ is quasi-reversible. There seems to have been no satisfactory theoretical treatment of a quasi-reversible polarographic wave for a two-electron process with distinct values of the standard potentials of the two steps. We have resorted to a steady-state solution[16,17] assuming linear diffusion, a model more appropriate to rotating-disk voltammetry.[18] Assuming that the first step is rate-limiting, we obtain

$$\frac{i}{i_d} = \frac{1 + \theta/2\theta'}{(1 + \theta/\theta')[1 + (k_d/k_0)(\theta\theta')^\alpha] + \theta^2} \quad (5)$$

where k_d is the mass transport rate constant and

$$\theta = \exp[F(E - E^\circ)/RT]$$

$$\theta' = \exp[F\Delta E/2RT]$$

(12) Nicholson, R. S.; Shain, I. *Anal. Chem.* **1964**, *36*, 706–723.
(13) Nicholson, R. S.; Shain, I. *Anal. Chem.* **1965**, *37*, 178–190.
(14) Digital simulation studies in our laboratories confirmed the form of eq 2 but showed that the reference point is the standard potential of the rate-limiting electron-transfer step.
(15) Isreal, Y.; Meites, L. *J. Electroanal. Chem. Interfacial Electrochem.* **1964**, *8*, 99–119.
(16) Albery, W. J. *Electrode Kinetics*; Oxford University Press: London, 1975.
(17) Rieger, P. H. *Electrochemistry*; Prentice-Hall: Englewood Cliffs, NJ, 1987.
(18) Rotating-disk voltammetric experiments were in qualitative agreement with this discussion, but the results were complicated by uncompensated ohmic potential drop and could not be analyzed quantitatively.

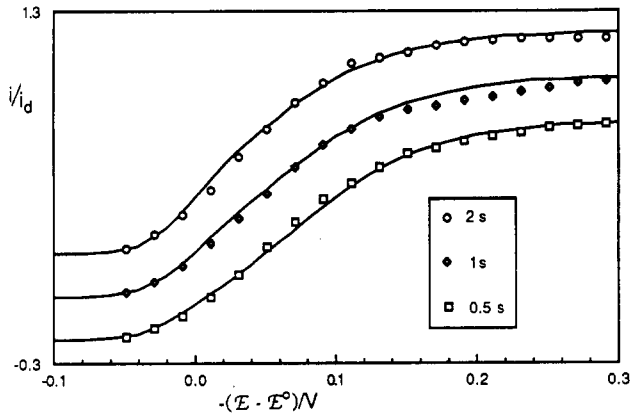

Figure 2. dc polarograms of $Ru_3(CO)_{12}$ in acetone for 0.5, 1.0, and 2.0 s drop times. Solid curves correspond to eq 8 with α = 0.52, $(k_d/k_0)(\theta')^\alpha$ = 4.10, 2.90, and 2.05 for t_d = 0.5, 1.0, and 2.0 s, respectively; plotted points are measured from experimental curves.

If $\Delta E > 100$ mV, then $\theta' \gg \theta$ in the vicinity of the wave and eq 5 can be simplified to

$$i_d/i = 1 + (k_d/k_0)(\theta\theta')^\alpha + \theta^2 \quad (6)$$

Equation 6 gives a good account of the shape of the observed polarographic waves, and a nonlinear least-squares fit of the wave shape provides estimates of $(k_d/k_0)(\theta')^\alpha$, α, and $E°$.[19] Polarograms with t_d = 0.5, 1.0, and 2.0 s were fitted in this way; the values of α and $E°$ were essentially the same for the three polarograms, but as expected from $k_d \approx (D/t_d)^{1/2}$, the fitted values of $(k_d/k_0)(\theta')^\alpha$ differed by approximately a factor of $2^{1/2}$. Assuming that the difference is exactly $2^{1/2}$, a single fit of all three polarograms, shown in Figure 2, gave α = 0.52 ± 0.02 and $(k_d/k_0)(\theta')^\alpha$ = 2.9 ± 0.4 (for t_d = 1.0 s) or

$$\Delta E + \frac{2RT}{\alpha F} \ln \frac{k_d}{k_0} = 0.103 \pm 0.015 \text{ V} \quad (7)$$

Combining eqs 7 and 3, assuming that $k_d \approx (D/t_d)^{1/2}$, we have another estimate of $E° = E_1° + \Delta E/2 = -1.49$ V, in satisfactory agreement with that obtained from an estimate of the limit of linearity of the cyclic voltammetry data.

Although we cannot separate ΔE from $D^{1/2}/k_0$, we can establish a plausible range: If $0.1 < \Delta E < 0.4$ V, eq 7 gives $1.0 > D^{1/2}/k_0 > 0.05$ $s^{1/2}$, or with $D \approx 10^{-5}$ cm^2 s^{-1}, $0.003 < k_0 < 0.06$ cm s^{-1}. A value of ΔE less than 0.1 V would lead to qualitative differences in polarographic wave shape, and a value larger than 0.4 V would require an implausibly large electron-transfer rate constant (remembering that electron transfer is coupled with Ru_3 ring opening). Thus with $E° = -1.5$ V, the first and second reduction potentials must be in the ranges $-1.55 > E_1° > -1.7$ V and $-1.45 < E_2° < -1.3$ V.

An analogous treatment of the ECE mechanism[17] leads to the following expression for the polarographic wave shape:

$$\frac{i}{i_d} = \frac{2 + \theta/\theta' - R}{(1 + \theta\theta' R)(2 - R)} \quad (8)$$

where $R = k_d(kD)^{-1/2}$. For a fast chemical step ($R \ll 1$) and $\Delta E > 100$ mV ($\theta' \gg \theta$), eq 8 reduces to $i_d/i = 1 + \theta\theta' R$, which corresponds to a normal symmetrical wave with $E_{1/4} - E_{3/4} = 56$ mV. Thus the polarographic results are also inconsistent with an uncomplicated ECE mechanism.

(19) Since a different reference electrode was used in the polarograms, the values of $E°$ are not directly comparable to that estimated above.

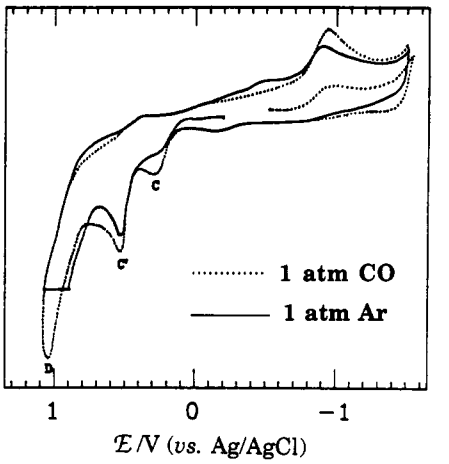

Figure 3. Cyclic voltammograms of 1 mM $K_2Ru_6(CO)_{18}$ (and ca. 0.15 mM $Ru_3(CO)_{12}$) in acetone: v = 600 mV s^{-1}, potentials vs Ag/AgCl reference. Solid curve: under 1 atm of Ar, initial positive-going sweep; dotted curve: under 1 atm of CO, initial negative-going sweep.

While our results seem to unambiguously support an EE mechanism, there are reasons for caution: (1) The primary electrode process is followed by one or more fast chemical steps (see below). If the dianion is consumed rapidly, then the rate-limiting first electron-transfer step is unaffected and our analysis should be qualitatively correct. However, if the radical anion is consumed by a homogeneous reaction, competitive with electron transfer, the analysis would be significantly perturbed. (2) An EC or ECE process may appear to have the chemical step concerted with electron transfer if the experimental method used involves a relatively long time scale.[20] Experiments with a shorter time scale might be capable of resolving the electron-transfer and ring-opening steps. For an ECE process with ΔE greater than a few hundred millivolts, the current wave necessarily occurs at $E > E_1°$. In order to appear electrochemically reversible, the first electron-transfer step would have to to unusually fast; even a moderately fast electron-transfer step might appear to be sufficiently irreversible to mask the effects of a separate chemical step.

The LUMO in $Ru_3(CO)_{12}$ has been shown by extended Hückel MO theory calculations[21] to be strongly metal–metal antibonding, consistent with ring opening concerted with or following electron transfer. Metal–metal bond cleavage on reduction in $Ru_3(CO)_{12}$ is analogous to that observed for $(R_2C_2)Co_2(CO)_6$,[22] except that in the case of the cobalt clusters, Co–Co bond cleavage in the anion radical occurs after reduction and is slow enough (k = 56 s^{-1} at 298 K for R = Ph) that the anion radical escapes from the electrode surface before significant further reduction occurs.

Oxidation of $K_2Ru_3(CO)_{11}$, $K_2Ru_6(CO)_{18}$, and $Ru(CO)_5$. Before proceeding to a discussion of the $Ru_3(CO)_{12}$ reduction products, we present the results of brief investigations of the electrochemical oxidation of the $Ru_3(CO)_{11}^{2-}$ and $Ru_6(CO)_{18}^{2-}$ anions and of mononuclear $Ru(CO)_5$.

$Ru(CO)_5$. Cyclic voltammograms of $Ru(CO)_5$ in acetone show an irreversible, multi-electron oxidation peak at +1.04

(20) Moraczewski, J.; Geiger, W. E. *J. Am. Chem. Soc.* **1981**, *103*, 4779–4787. Grzeszczuk, M.; Smith, D. E.; Geiger, W. E. *J. Am. Chem. Soc.* **1983**, *105*, 1772–1776.

(21) Tyler, D. R.; Levenson, L. A.; Gray, H. B. *J. Am. Chem. Soc.* **1978**, *100*, 7888–7893.

(22) Arewgoda, M.; Rieger, P. H.; Robinson, B. H.; Simpson, J.; Visco, S. J. *J. Am. Chem. Soc.* **1982**, *104*, 5633–5640.

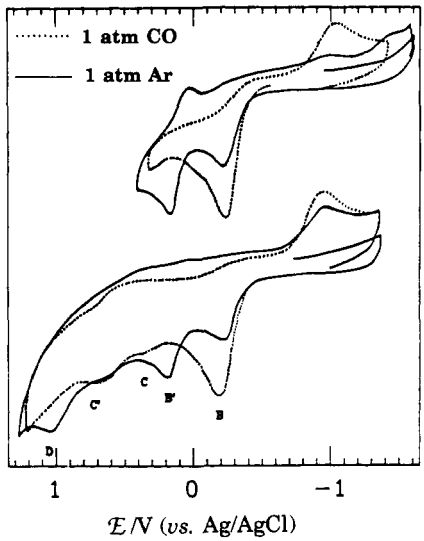

Figure 4. Cyclic voltammograms of 1 mM $K_2Ru_3(CO)_{11}$ in acetone: v = 600 mV s^{-1}, potentials vs Ag/AgCl reference. Solid curves: under 1 atm of Ar, initial negative-going sweep; dotted curves: under 1 atm of CO, initial positive-going sweep.

V vs Ag/AgCl (D).[23] On the reverse cathodic scan, a small irreversible reduction peak is seen at −0.21 V. At −50 °C, the oxidation is unchanged, but several additional reduction peaks are observed in the range −0.2 to −1.2 V.

$Ru_6(CO)_{18}^{2-}$. Figure 3 shows a cyclic voltammogram of $K_2Ru_6(CO)_{18}$ in acetone. Although the sample contained about 15% $Ru_3(CO)_{12}$, it is clear that peaks C (+0.25 V), C′ (+0.52 V) and D (ca. 1.0 V) can be attributed to $Ru_6(CO)_{18}^{2-}$, with peak current ratios approximately 1:3:5. When the scan includes peak D, a reduction peak is observed at −0.52 V; this peak grows on successive cycles while C diminishes in size.

Under 1 atm of CO, the peak C current approximately doubles and is not affected when the scan includes peak D; the −0.52 V reduction is not observed and the $Ru_3(CO)_{12}$ reduction peak is substantially enhanced.

$K_2Ru_3(CO)_{11}$. dc polarograms of $K_2Ru_3(CO)_{11}$ in acetone show two rather poorly defined oxidation waves. Comparison of the limiting current with that of benzoquinone suggests that both oxidation steps involve one electron.

Cyclic voltammograms of $K_2Ru_3(CO)_{11}$ in acetone (Figure 4) show irreversible oxidations at −0.22 (B), +0.17 (B′), and +1.01 V (D) with approximately equal peak currents. If the potential sweep is reversed after peak D, the $Ru_3(CO)_{12}$ reduction peak is observed at −0.92 V as well as a second major reduction peak at −1.37 V. If the potential scan is switched just after B′ (Figure 4) the $Ru_3(CO)_{12}$ reduction is much smaller and oxidation B′ appears to be partially reversible.

The cyclic voltammogram of $K_2Ru_3(CO)_{11}$ changes dramatically in the presence of CO: (i) The peak B current doubles. (ii) Peak B′ disappears, and peak D is only barely detectable. (iii) Small oxidation peaks are observed at +0.26 V (C) and +0.56 V (C′), suggesting the formation of $Ru_6(CO)_{18}^{2-}$. (iv) The $Ru_3(CO)_{12}$ reduction is much larger and is observed even if the potential scan is reversed just after peak B. (v) The −1.37-V reduction peak is much smaller.

Clearly oxidation of $Ru_3(CO)_{11}^{2-}$ leads to a complex group of chemical reactions, probably including fragmentation to $Ru(CO)_5$, for which peak D is characteristic. The addition of CO apparently reduces the pathways to a major reaction leading to $Ru_3(CO)_{12}$—the ECE process of Scheme III—and a minor reaction leading to $Ru_6(CO)_{18}^{2-}$. It is tempting to suggest formation of $Ru_6(CO)_{18}^{2-}$ through the reaction of $Ru_3(CO)_{12}$ with $Ru_3(CO)_{11}^{2-}$; this reaction apparently is feasibly energetically, but it is probably too slow to make a significant contribution on the CV time scale. It is more likely that $Ru_3(CO)_{12}$ reacts with the radical anion intermediate, $Ru_3(CO)_{11}^{-}$, followed by a one-electron reduction and loss of 5 mol of CO, Scheme IV.

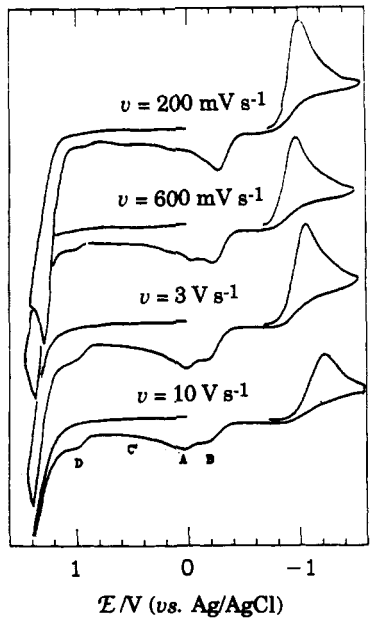

Figure 5. Cyclic voltammograms of 1 mM $Ru_3(CO)_{12}$ in acetone: v = 200 mV s^{-1} (current × 10), 600 mV s^{-1} (current × 5), 3 V s^{-1} (current × 2.5), 10 V s^{-1} (current × 1); potentials vs Ag/AgCl reference.

Scheme III

$$Ru_3(CO)_{11}^{2-} - e^- \rightleftarrows Ru_3(CO)_{11}^{\bullet -}$$

$$Ru_3(CO)_{11}^{\bullet -} + CO \rightarrow Ru_3(CO)_{12}^{\bullet -}$$

$$Ru_3(CO)_{12}^{\bullet -} - e^- \rightleftarrows Ru_3(CO)_{12}$$

Scheme IV

$$Ru_3(CO)_{11}^{2-} - e^- \rightleftarrows Ru_3(CO)_{11}^{\bullet -}$$

$$Ru_3(CO)_{11}^{\bullet -} + Ru_3(CO)_{12} \rightarrow Ru_6(CO)_{23-x}^{\bullet -} + xCO$$

$$Ru_6(CO)_{23-x}^{\bullet -} + e^- \rightleftarrows Ru_6(CO)_{18}^{2-} + (5-x)CO$$

Secondary Oxidation Processes following Reduction of $Ru_3(CO)_{12}$. Several oxidation peaks are observed in cyclic voltammograms of $Ru_3(CO)_{12}$ in acetone solutions (Figure 5). Some of these can be assigned with some confidence: Thus the feature at −0.22 V (B) is due to *trangulo*-$Ru_3(CO)_{11}^{2-}$, and the feature at ca. +1.0 V (D), to $Ru(CO)_5$. $Ru_3(CO)_{12}$ itself undergoes a chemically irreversible three-electron oxidation at about +1.3 V. A minor feature (C′) is sometimes seen (it is always present on the second and subsequent cycles) at ca. +0.52 V, which can be assigned to $Ru_6(CO)_{18}^{2-}$.

Neither we nor Robinson et al.[7] observed the second oxidation peak characteristic of $Ru_3(CO)_{11}^{2-}$ (B′) in cyclic voltammograms of $Ru_3(CO)_{12}$. The CO concentration in the vicinity of the electrode is apparently sufficiently high that oxidation of $Ru_3(CO)_{11}^{2-}$ involves two electrons—the

(23) Unless otherwise noted, all peak potentials in this section are relative to the Ag/AgCl/acetone reference electrode and refer to room-temperature cyclic voltammograms at a scan rate of 600 mV s^{-1}.

ECE process of Scheme III.[24]

As might be expected from the cyclic voltammogram of $Ru_6(CO)_{18}^{2-}$, peak C is never detectable in cyclic voltammograms of $Ru_3(CO)_{12}$, but peak C′ sometimes can be seen at slower scan rates ($v < 10$ V s^{-1}) with a peak current up to about 5% that of the primary reduction. Not surprisingly—$Ru_6(CO)_{18}^{2-}$ necessarily arises through a bimolecular process—neither C nor C′ can be seen for $[Ru_3(CO)_{12}] < 0.3$ mM.

Peaks C′ and D are not observed in cyclic voltammograms of $Ru_3(CO)_{12}$ at low temperatures or at fast scan rates. Indeed, these features are only seen when peak B is prominent. Since C′ and D are also seen in cyclic voltammograms of $K_2Ru_3(CO)_{11}$, $Ru_6(CO)_{18}^{2-}$ and $Ru(CO)_5$ may be products of the oxidation of $Ru_3(CO)_{11}^{2-}$ rather than of the reduction of $Ru_3(CO)_{12}$.

The other significant feature in the cyclic voltammograms of $Ru_3(CO)_{12}$ in acetone is the oxidation peak at −0.09 V (A). In the following, we discuss several hypotheses regarding the identity of this feature.

(1) Open-Chain Dianion. In our earlier paper,[6] we assigned A to oxidation of the primary reduction product, open-chain $Ru_3(CO)_{12}^{2-}$. The basis for our assignment was that, in acetone, A is the major oxidation peak at fast scan rates and is the only oxidation observed at low temperatures. The ratio of peak heights, B:A, decreases with increasing CO pressure, but the sum of A + B, is essentially unaffected by CO; accordingly, we postulated reversible CO loss from $Ru_3(CO)_{12}^{2-}$, followed by irreversible cyclization to give $Ru_3(CO)_{11}^{2-}$ (B). There are two reasons for rejecting this interpretation: (i) The detailed dependence of the B:A peak current ratio on scan rate is inconsistent with a single first-order process (see below) and (ii) the potential of peak A, −0.09 V, is inconsistent with our estimate of $E_2°$ (−0.64 to −0.79 vs Ag/AgCl). On the other hand, the peak observed by Robinson et al.[7] in dry CH_2Cl_2 (−0.6 V, assigned to the oxidation of $Ru_3(CO)_{12}^{2-}$) is entirely consistent with our estimate of $E_2°$. Thus we are forced to the conclusion that A is not $Ru_3(CO)_{12}^{2-}$ and that this species, if it is formed in acetone, is very rapidly consumed by one or more processes which lead to species A, as well as to $Ru_3CO)_{11}^{2-}$.

(2) Product of a Reaction with Water. Although peak A was not observed in Robinson's work with CH_2Cl_2 under rigorously dry conditions, some of our cyclic voltammograms of $Ru_3(CO)_{12}$ in CH_2Cl_2, carefully dried but exposed to the atmosphere during solution preparation, exhibited a small feature resembling A, but only 70–100 mV more positive than B (the B/A separation is 130–180 mV in acetone). Robinson et al. presented evidence suggesting that water is involved in the formation of $Ru_3(CO)_{11}^{2-}$ in CH_2Cl_2. These results suggested that A might be due to the product of a reaction of $Ru_3(CO)_{12}^{2-}$ with water. Addition of water up to ca. 1 M had very little effect on B (or on A at 10 V s^{-1}) but decreased the size of A by 20–30% at slow scan rates ($v < 2$ V s^{-1}). It would appear that, for acetone solutions, the species responsible for A does not result from a reaction of water; indeed, it apparently reacts with water.

(3) Ru_6 Species. Robinson's observation that the −0.6-V peak disappears at $Ru_3(CO)_{12}$ concentrations greater than 0.1 mM suggests that, at least in CH_2Cl_2 solutions, $Ru_3(CO)_{12}^{2-}$ is consumed in a bimolecular reaction. The appearance of $Ru_6(CO)_{18}^{2-}$ as a minor product of reduction of $Ru_3(CO)_{12}$ in both acetone and CH_2Cl_2 reductions of $Ru_3(CO)_{12}$ seems to support this hypothesis, although, as

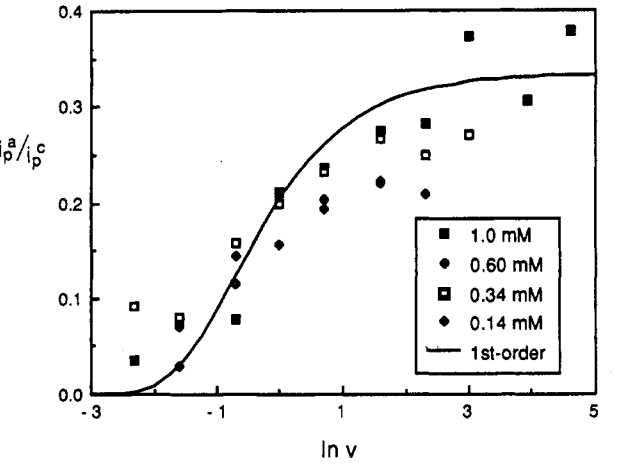

Figure 6. Peak current of oxidation peak A, normalized to the current of the primary reduction peak, as a function of scan rate. The solid line represents the behavior expected for a first-order decay process with $k = 0.5$ s^{-1} and a zero-time peak current ratio of 1:3.

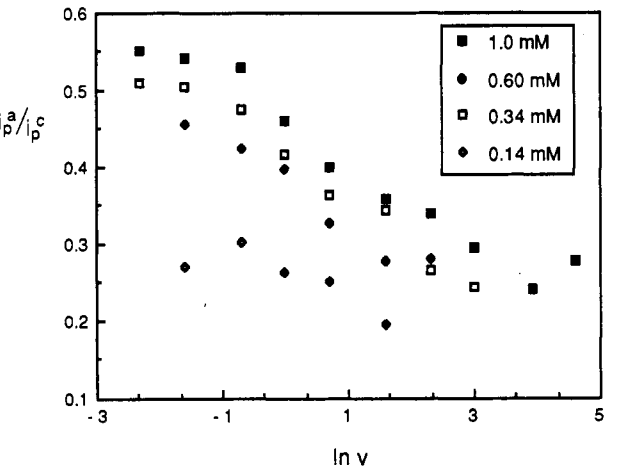

Figure 7. Peak current of oxidation peak B, normalized to the current of the primary reduction peak, as a function of scan rate.

pointed out above, $Ru_6(CO)_{18}^{2-}$ could arise solely from the oxidation of $Ru_3(CO)_{11}^{2-}$. Accordingly, we considered a mechanism in which A and B arise through competitive first- and second-order processes, Scheme V. Since peak

Scheme V

$$Ru_3(CO)_{12}^{2-} \overset{\text{fast}}{\rightleftharpoons} Ru_3(CO)_{11}^{2-}\ (B) + CO$$

$$Ru_3(CO)_{12}^{2-} + Ru_3(CO)_{12} \xrightarrow{\text{fast}} Ru_6(CO)_{24-x}^{2-}\ (A) + xCO$$

$$Ru_6(CO)_{24-x}^{2-} \xrightarrow{\text{slow}} Ru_6(CO)_{18}^{2-} + \text{other products}$$

C′ ($Ru_6(CO)_{18}^{2-}$) never amounts to more than a few percent of the total oxidation current, the last step mostly yields "other products". This scheme comes closer to explaining the dependence of the A:B peak current ratio on scan rate.[25] However, this mechanism predicts that the peak A current should be strongly concentration-dependent. In Figures 6 and 7, we show the A and B peak currents, relative to that of the primary cathodic peak, for 0.14, 0.34, 0.60, and 1.0 mM $Ru_3(CO)_{12}$ in acetone for a series of cyclic voltammograms measured under identical conditions.[26]

(24) CO necessarily is produced along with $Ru_3(CO)_{11}^{2-}$, and it may also be a byproduct of the production of species A.

(25) See Figure 8 in: Gosser, D. K.; Rieger, P. H. *Anal. Chem.* **1988**, *60*, 1159–1167.

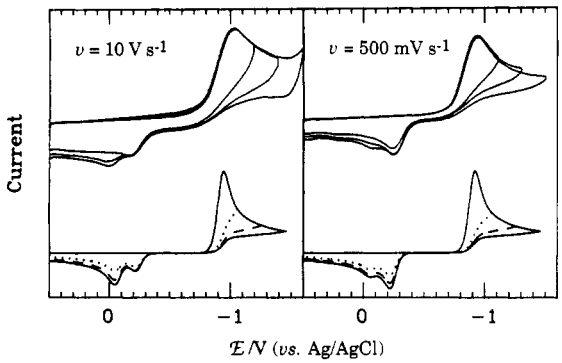

Figure 8. Cyclic voltammograms of 0.6 mM $Ru_3(CO)_{12}$ in acetone (upper) at 10 V s^{-1} and 0.5 V s^{-1} showing the effects of changing the switching potential and digital simulations (lower) for reversible one-electron electrode processes showing the effect of the homogeneous reactions of Scheme VI, $k_1 = 400\ s^{-1}$, $k_2 = 1.2 \times 10^6\ M^{-1}\ s^{-1}$, $k_3 = 1\ s^{-1}$.

The scan rate dependence of peak A suggests a relatively slow first-order decay process ($k \approx 0.5\ s^{-1}$), but the peak A current shows no significant concentration dependence, suggesting that A is formed very rapidly by a process first-order in Ru_3 cluster. For a given concentration, the sum of the A and B peak currents is roughly constant, suggesting that A does indeed convert to B. However, the B peak current does not approach zero at fast scan rates and is somewhat dependent on concentration, suggesting that $Ru_3(CO)_{11}^{2-}$ is formed both by a first-order reaction of A and more directly from $Ru_3CO)_{12}^{2-}$, perhaps by a process second-order in Ru_3 cluster.

(4) First-Order Product in a Competitive Reaction Scheme. These conclusions can be summarized in the phenomenological mechanism of Scheme VI, where "Ru_3"

Scheme VI

$$Ru_3(CO)_{12}^{2-} \xrightarrow{k_1} A$$

$$Ru_3(CO)_{12}^{2-} + \text{"}Ru_3\text{"} \xrightarrow{k_2} Ru_3(CO)_{11}^{2-} + ?$$

$$A \xrightarrow{k_3} Ru_3(CO)_{11}^{2-}$$

could be $Ru_3(CO)_{12}$, $Ru_3(CO)_{12}^{\bullet-}$, or $Ru_3(CO)_{12}^{2-}$. The first two reactions are very fast; the third, relatively slow, $k_3 \approx 0.5\ s^{-1}$. One of the two reactions forming $Ru_3(CO)_{11}^{2-}$ must be reversible and produce CO in order to account for the effects described above.

Scheme VI accounts, at least qualitatively, for the scan rate and concentration dependences of the A and B peak currents. It also accounts for the effect of the CV switching potential on the A and B peak currents, shown in Figure 8. At slow scan rates (<1 V s^{-1}), both the A and B peak currents increase as the switching potential is made more negative. At fast scan rates, however, the B peak current is nearly independent of switching potential. In general, the longer the cathodic electrolysis continues, the bigger a product oxidation peak. When there is a single reaction, this is true regardless of the order of the reaction, but in a competitive situation, there is an important difference. The electrode surface concentrations of $Ru_3(CO)_{12}$, $Ru_3(CO)_{12}^{\bullet-}$, and $Ru_3(CO)_{12}^{2-}$—the prospective second-order reactants—fall rapidly when the potential scan passes the cathodic current peak, so that the first-order process must dominate in the falling portion of the current peak. The second-order products then are formed mostly in the rising portion of the current peak; thus the yield of second-order products is nearly independent of switching potential. According to Scheme VI, B arises mostly through the second-order process at fast scan rates but increasingly via species A as the scan rate decreases. This interpretation is confirmed by digital simulations, as shown in Figure 8.

While digital simulation studies have provided qualitative support for Scheme VI, they have also convinced us that quantitative interpretation would be very difficult. In dealing with products of a fast reaction following reduction of substrate, it is usually sufficient to know that the process is fast on the CV time scale; the size of subsequent oxidation peaks then are more or less independent of the rate of the reaction. Here, however, competition between first- and second-order processes results in a complex interaction of the two rate constants and the scan rate, which would require simulations using the true (very fast) rates to obtain results that accurately mirror experiments. The simulations shown in Figure 8 used $k_1 = 400\ s^{-1}$, $k_2 = 1.2 \times 10^6\ M^{-1}\ s^{-1}$, and $k_3 = 1\ s^{-1}$, but these should be regarded as illustrative at best. The true rate constants, k_1 and k_2, are certainly larger than these values and probably have a very different ratio; k_3 is probably closer to $0.5\ s^{-1}$.

(5) Solvent Adduct. At this point we cannot definitively identify species A in Scheme VI, but an attractive candidate is the nucleophilic substitution product, $Ru_3(CO)_{11}S^{2-}$, where S is either acetone or water, with the water derivative having a somewhat shorter lifetime. This hypothesis is consistent with the total absence of peak A in carefully dried CH_2Cl_2, its ubiquitity in acetone solutions, and the somewhat different potential of A in acetone and undried CH_2Cl_2, and it could be consistent with Scheme VI. Since A is observed in acetone at low temperatures and at very fast scan rates, it must be formed by a very fast reaction. It is tempting to postulate nucleophilic substitution of acetone for CO at the monoanion stage, in competition with electron transfer. While this cannot be entirely ruled out, it seems unlikely that such a high yield would be obtained under all conditions. On the other hand, it would be surprising that the rate of substitution of acetone for CO in $Ru_3(CO)_{12}^{2-}$ should be very fast, and also surprising that $Ru_3(CO)_{11}S^{2-}$ would be harder to oxidize than $Ru_3(CO)_{12}^{2-}$. Nonetheless, this assignment seems the most likely identification of species A.

Experimental Section

Materials. Tetrahydrofuran (THF) was dried over CaH_2 for 25 h and then distilled from sodium benzophenone ketyl. Methylene chloride was dried over activated molecular sieves (3A) and then distilled from P_2O_5 on a vacuum line. Hexanes, pentane, and acetone were Fisher reagent grade and were dried over activated molecular sieves (3A or 4A).

Tetrabutylammonium perchlorate (TBAP) was obtained from Southwestern Analytical Chemicals as the hydrate, recrystallized from ethyl acetate/pentane, and vacuum-dried over P_2O_5. Tetrabutylammonium tetrafluoroborate (TFAFB) was prepared according to Ross,[27] recrystallized twice from methanol/water, and vacuum-dried over P_2O_5.

$Ru_3(CO)_{12}$ was obtained from Strem or Aldrich and recrystallized from hexanes prior to use. $K_2Ru_3(CO)_{11}$ and $K_2Ru_6(CO)_{18}$ were prepared by the reduction of $Ru_3(CO)_{12}$ with potassium benzophenone ketyl in THF following the methods of Shore.[8] Infrared spectra (Digilab FTS-15B or Perkin-Elmer 681) of these products in THF solution: for $Ru_3(CO)_{11}^{2-}$, ν (cm^{-1}) = 2033 (w),

(26) Peak A currents were corrected for overlap with peak B, assuming $t^{-1/2}$ dependence for peak B and a constant 180-mV separation of the two peaks.

(27) Ross, S. D.; Rudd, E. J.; Finkelstein, M. *J. Org. Chem.* **1972**, *37*, 1763–1767.

2018 (vw), 1990 (w, sh), 1964 (s), 1948 (vs), 1920 (s), 1896 (m, sh), 1653 (m); for $Ru_6(CO)_{18}^{2-}$, $\tilde{\nu}$ (cm^{-1}) = 2003 (vs), 1986 (vs), 1963 (m, sh), 1937 (m, sh), plus weak bands attributable to about 15% unreacted $Ru_3CO)_{12}$ (2060 and 2030 cm^{-1}). $Ru(CO)_5$ was prepared from $Ru_3(CO)_{12}$ by the photochemical method of Lewis et al.,[28] purified by vacuum line distillation, and stored under CO in a freezer until use. Infrared bands were observed at $\tilde{\nu}$ (cm^{-1}) = 2036 (s), 2004 (vs).

Solutions for electrochemical studies were freshly prepared from the reagents purified as described above. Unless otherwise specified, such solutions were 1.0 mM in the electroactive compound and 0.15 M in supporting electrolyte and were deoxygenated with and kept under argon during the experiments.

Electrochemical Measurements. dc polarograms were recorded with a PAR 174 polarographic analyzer in the three-electrode configuration with *iR*-drop compensation. Cyclic voltammograms, recorded on a Bascom-Turner 2120 digital recorder (for $v \geq 200$ mV s^{-1}) or on a Hewlett-Packard x-y recorder (for slower scan rates), employed a Pt-wire counter electrode, a Ag/AgCl reference electrode making contact with the solution through a Luggin probe, and a Pt-button (ca. 2 mm diameter) working electrode. The Pt working electrode was surface polished and anodized in a solution of the supporting electrolyte for 45 s at +2.0 V before use. The reference electrode contained a Ag/AgCl reference element with 0.1 M TBAP in acetone, saturated in LiCl ($E_{1/2}$ = 0.66 V for ferrocene in acetone solution with 0.1 M TBAP). Low-temperature work in CH_2Cl_2 used a Ag/AgCl electrode with 0.1 M TBAFB in CH_2Cl_2, saturated in LiCl ($E_{1/2}$ = 0.60 V for ferrocene in CH_2Cl_2 solution with 0.1 M TBAFB). Unless otherwise noted, potentials reported here are relative to the acetone Ag/AgCl electrode.

Room-temperature cyclic voltammograms were obtained by using a standard BAS cell. Cyclic voltammograms at −56 °C employed a jacketted cell and acetone coolant circulated through a dry ice/acetone bath. Cyclic voltammograms at −90 °C were recorded with a Metrohm cell immersed in a liquid nitrogen/CH_2Cl_2 slush bath.

In a series of experiments in which the potential of the $Ru_3(CO)_{12}$ reduction peak was measured as a function of scan rate, the solutions contained an equimolar concentration of ferrocene; the separation of the ferrocene oxidation and reduction peaks were used to estimate the solution resistance, which was used to correct the $Ru_3(CO)_{12}$ reduction peak potentials for ohmic potential drop in the solution.

(28) Johnson, B. F. G.; Lewis, J.; Twigg, M. V. *J. Organomet. Chem.* **1974**, *67*, C75–C76. *J. Chem. Soc., Dalton Trans.* **1975**, 1876–1879.

Direct Electrochemical Synthesis of X_2InCH_2X Compounds (X = Br, I) and a Study of Their Coordination Chemistry

Theodore A. Annan and Dennis G. Tuck*

Department of Chemistry and Biochemistry, University of Windsor, Windsor, Ontario, Canada N9B 3P4

Masood A. Khan

Department of Chemistry, University of Oklahoma, Norman, Oklahoma 73019

Clovis Peppe

Departamento de Quimica, CCEN, Universidade Federal da Paraiba, Cidade Universitaria, 58000 J. Pessoa-PB, Brazil

Received October 26, 1990

The electrochemical oxidation of indium in CH_2X_2/CH_3CN media (X = Cl, Br, I) gives InX. Indium(I) chloride disproportionates, but InBr or InI react with CH_2X_2 to give X_2InCH_2X (X = Br, I) derivatives. Treatment of the latter with Et_4NX gives the 1:1 electrolytes $Et_4N[X_3InCH_2X]$. With triphenylphosphine, Br_2InCH_2Br forms the phosphonium ylid derivative $Br_3InCH_2P(C_6H_5)_3$, whose structure has been established by X-ray crystallography: cell constants a = 14.076 (4) Å, b = 7.610 (2) Å, c = 12.931 (2) Å; space group $Pna2_1$; R = 0.034, R_w = 0.034. Reaction between *N,N,N',N'*-tetramethylethanediamine (tmen) and Br_2InCH_2Br also gives a cyclized nitrogen ylid $Br_3\overline{InCH_2NMe_2CH_2NMe_2}$: cell constants a = 12.814 (3) Å, b = 15.721 (4) Å, c = 21.343 (5) Å; space group $Pbca$; R = 0.045, R_w = 0.047. The iodo species I_2InCH_2I undergoes redistribution in solution, and two tmen derivatives were isolated, $I_3\overline{InCH_2NMe_2CH_2NMe_2}$ and $[\overline{IIn(CH_2NMe_2CH_2NMe_2)_2}](I)_2$. The latter has two identical cyclized ylid ligands: a = 11.414 (4) Å, b = 14.592 (6) Å, c = 16.144 (7) Å, β = 110.1 (4)°; space group $P2_1/c$; R = 0.051, R_w = 0.051. The ^1H and ^{13}C NMR spectra show that the CH_2 group in X_2InCH_2X is electron-poor, in keeping with the tendency for nucleophilic ligands to react at this site as well as at the metal.

Introduction

The method of direct electrochemical synthesis consists of oxidizing a metal anode in a nonaqueous solution containing a ligand or ligand precursor to produce the appropriate metal–ligand complex. One of the many advantages of the technique is that the compound is often a derivative of a low oxidation state of the metal in question, and examples of this include chromium(III) bromide.[1] tin(II) and lead(II) thiolates,[2] hexahalogenodigallate(II) anions,[3] thorium diiodide,[4] copper(I) thiolates,[5] and indium(I) derivatives of thiols,[6] dithiols,[7] and diols.[8]

* To whom correspondence should be addressed.

(1) Habeeb, J. J.; Tuck, D. G. *Inorg. Synth.* **1979**, *19*, 123.
(2) Hencher, J. L.; Khan, M. A.; Said, F. F.; Sieler, R.; Tuck, D. G. *Inorg. Chem.* **1982**, *21*, 2787.
(3) Khan, M. A.; Taylor, M. J.; Tuck, D. G.; Rogers, D. A. *J. Crystallogr. Spectrosc. Res.* **1986**, *16*, 895.
(4) Kumar, N.; Tuck, D. G. *Inorg. Chem.* **1983**, *22*, 1951.
(5) Chadha, R. K.; Kumar, R.; Tuck, D. G. *Can. J. Chem.* **1987**, *65*, 1336.

0276-7333/91/2310-2159$02.50/0